Journal of Organometallic Chemistry 695 (2010) 2596–2602

Contents lists available at ScienceDirect

Journal of Organometallic Chemistry

journal homepage: www.elsevier.com/locate/jorganchem

The influence of nitrogen sources on nitrogen doped multi-walled carbon nanotubes

Edward N. Nxumalo [a], Phatu J. Letsoalo [b], Leskey M. Cele [b], Neil J. Coville [a,*]

[a] DST/NRF Center for Excellence in Strong Materials and Molecular Sciences Institute, School of Chemistry, University of the Witwatersrand, WITS 2050, Johannesburg, South Africa
[b] DST/NRF Center for Excellence in Strong Materials and Department of Chemistry, University of Johannesburg, Doornfontein, P.O. Box 17011, 2028, Johannesburg, South Africa

ARTICLE INFO

Article history:
Received 6 May 2010
Received in revised form
5 August 2010
Accepted 20 August 2010
Available online 21 September 2010

Keywords:
Nitrogen doped carbon nanotubes
Nitrogen containing reagents
Ferrocene
Sonication

ABSTRACT

A range of nitrogen doped carbon nanotubes (N-CNTs) was produced by a nebulised floating catalyst method at 850 °C using a mixture of toluene and 1–8% nitrogen containing reagents (a range of amines and amides). The carbon nanotube (CNT) products were characterized by transmission electron microscopy (TEM), scanning electron microscopy (SEM) and thermogravimetric analysis (TGA), CHN analysis as well as Raman spectroscopy. Differences due to the different N containing reagents were noted but in general all reagents gave aligned CNTs that at low concentration (1%) were longer and wider than those produced without nitrogen. Increased N content in the reactant mixture gave doped tubes that became shorter and showed more disorder. Treatment of the N-CNTs with nitric acid (microwave, 30 min) gave samples that were chemically modified by the acid (loss of alignment, narrower tubes and more facile oxidation). *It appears in general that the amount of N in the nitrogen containing reagent is more important than the source and type of the N atoms used as revealed by trends in the morphology (diameter, length) of the N-CNTs produced.*

1. Introduction

The synthesis and characterization of nitrogen doped carbon nanotubes (N-CNTs) have been extensively investigated over the last decade [1,2]. This is due to the enhancement in particular of the electronic structure of carbon nanotubes (CNTs) upon the insertion of N into the CNT lattice [3,4]. N-doping has been proven to be a feasible strategy to tailor the electronic properties of CNTs in a well defined manner [5,6]. Due to their enhanced catalytic properties, N-CNTs have been used as catalyst supports in oxidation reactions [7] and for proton-exchange fuel cells [8].

Several workers have reported on the growth of N-CNTs using chemical vapour deposition (CVD) approaches. This is demonstrated by the considerable number of literature reviews that exist in this field [9–12]. Investigations indicate that N incorporation into CNTs strongly depends on the synthesis conditions used, such as the precursor, catalyst, reaction temperature as well as the gas flow rate. Several nitrogen containing reagents have been used to make N-CNTs [13–22]. Floating catalyst CVD methods are normally preferred for these reactions and ferrocene (FcH) and $Fe(CO)_5$ have been usually employed as catalysts [14,23,24]. The choice of the catalyst and N source are highly dependent on ease of use, availability, cost and volatility.

It is now well known that N-CNTs demonstrate characteristic morphological features normally referred to as compartmentalized bamboo structures [25–27]. Indeed, doping with N also leads to more disorder in a tube through an increase in the number of defects created [28]. Furthermore, the number of walls in a CNT decreases when N is incorporated into CNTs. However, the correlation between the morphology and the type of N source used is not fully understood. Reports reveal that the pyrolysis of a carbon source and a nitrogen source in the CVD reactor (under appropriate experimental conditions) leads to the formation of N-CNTs. While the role of different types of carbon sources has been investigated, the role of the source and type of N has not been described.

To explore the role of using different N types and sources we report here a *systematic study* of N-CNTs, synthesized with a wide range of N containing reactants using a range of reagent concentrations (1–8%) to evaluate the effect of the N source and concentration on the new N-CNT materials. The range of nitrogen containing complexes studied includes amines and amides attached to a range of carbon functionalities (*i.e.* alkyl groups, aryl groups, etc.).

* Corresponding author. Tel.: +27 11 717 6738; fax: +27 11 717 6749.
E-mail address: neil.coville@wits.ac.za (N.J. Coville).

0022-328X/$ – see front matter © 2010 Elsevier B.V. All rights reserved.
doi:10.1016/j.jorganchem.2010.08.030

2. Experimental

2.1. Synthesis of doped CNTs

Carbon nanotubes were synthesized using the experimental setup shown in Fig. S1. In a typical synthesis, approximately 2.0 g of FcH, was dissolved in a mixture of 50 ml of a nitrogen containing hydrocarbon and toluene. The solution, nebulized using a 1.45 MHz oscillator, was carried into a 25 mm diameter quartz tube, placed in a furnace which was maintained at a temperature of 850 °C. The average droplet size for the solvents is ~2.2 μm at 1.54 MHz frequency [29]. The nitrogen containing hydrocarbons (diethylamine, butylamine, isopropylamine, benzylamine, *N*-benzylmethylamine, aniline, 1-methylpiperazine, hexamethylenediamine, trimethylenediamine, *N*-methylenediamine pyridine, quinoline, formamide, *N,N*-dimethylformamide, *N,N*-dimethylacetamide) were used as purchased (Sigma Aldrich and Fluka) and studied at concentrations of 1%, 2%, 4%, 6% and 8% in toluene. Ultra pure argon and hydrogen gases purchased at Afrox were used as the carrier gases and the gas flow rate was controlled using unit mass flow controllers.

In a typical procedure, the carrier gas flow rate was kept at 400 sccm (argon) and 100 sccm (hydrogen) respectively. The pyrolysis was carried out for 45 min. After the reaction, the argon flow rate was reduced to between 50 and 60 sccm whilst the flow rate of hydrogen was switched off. The furnace was then allowed to cool to room temperature. The products were collected after the reaction tube has cooled to room temperature. The yields were determined by scraping the products from the reactor and weighing. Errors of <10% can be expected in the yields, and trends are readily detected in the series of reactions performed.

2.2. Carbon nanotube analysis

Transmission electron microscopy (TEM) was performed on a JEM − 100S TEM instrument operating at 80 keV. Sample preparation for TEM studies involved sonicating approximately 0.09 g of sample in 10 ml of methanol for approximately 10 min. A few drops of the resulting suspension were placed on a holey carbon TEM grid, after which TEM images were recorded. A scanning electron microscope (SEM) (JOEL-JSM-5600 operated at 15 keV) was used to observe the morphology of the carbon nanotube arrays and to measure the average multi-wall CNT (MWCNT) length that was determined from the thickness of the nanotube arrays. Thermogravimetric analysis (TGA) was performed using a Perkin Elmer Pyris Thermogravimetric Analyzer 1 TGA under air at a flow rate of 25 ml/min. The samples were ramped from room temperature to 800 °C at a heating rate of 10 °C/min for the dynamic analysis. The sample weight used was approximately 5 mg. The laser Raman spectra were obtained from a Jobin Yvon T6400 laser Raman spectrometer operated in single spectrograph mode with a 600 line/nm grating. The 514.5 nm line of an argon ion laser was used as an excitation source. The laser power of the sample was kept at 1.2 mW or less to minimize local heating. Spectra were collected using a liquid nitrogen-cooled CCD detector (accumulation time varied from 120 to 180 s).

2.3. Acid washing of the N-CNTs

Reaction of the nanotube samples (about 50 mg) with concentrated nitric acid (5 ml) was accomplished by placing the samples in a closed vessel inside a microwave oven (CEM Microwave Technology). An oven power of 100 W was used for 30 min. CNTs prepared from the pyrolysis of toluene/FcH and from the pyrolysis of toluene/FcH in the presence of diethylamine (1%, 8%), quinoline (8%), hexamethylenediamine (1%) and *N,N*-dimethylacetamide (1%, 8%) were studied. After microwave treatment, the mixtures were washed with de-ionized water. The purified CNTs were then dried in a thermal oven at temperatures of about 100 °C. The morphologies of the purified N-CNTs were characterized by SEM, TEM, TGA and Raman spectroscopy.

3. Results and discussion

3.1. N-CNT yields

N-doped carbon nanotubes were synthesized by nebulized spray pyrolysis using approximately 2.0 g of FcH dissolved in 50 ml of toluene and nitrogen containing organic compounds at concentrations of 1%, 2%, 4%, 6% and 8%. Standard reaction conditions were chosen so that a comparison of the effect of the different nitrogen donors on the yield and morphology of the CNTs could be made.

The yield of CNTs synthesized in toluene without the addition of nitrogen containing organic compounds (0.70 g) provided a standard to evaluate the effect of the nitrogen on the reaction. The yield of CNTs obtained using the different reactants are given in Table S1 (Supplementary material section). In addition, two graphical examples of the yield data are shown in Fig. 1 and Fig. S2 that enables the data to be readily visualized.

An initial increase in mass relative to FcH/toluene (0.70 g) reagents is observed *in every case* when 1% of nitrogen containing hydrocarbons were added during the synthesis of the CNTs. The effect of increasing the concentration of the nitrogen containing reagent however varies with the reagent. Observations derived from information contained in Table S1 are listed below:

(i) For the amines (diethylamine, isopropylamine, butylamine, benzylamine) the yield of CNTs generally decreases with increase in amine concentration eventually producing yields

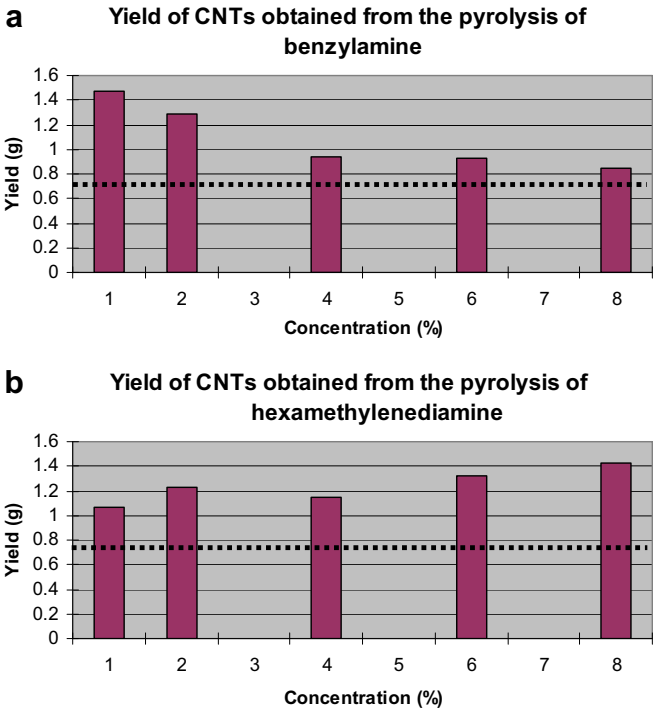

Fig. 1. Graphical representation of CNT yields grown from (a) benzylamine; and (b) hexamethylenediamine. Horizontal dotted line indicates yield of CNTs obtained from FcH/toluene.

close to or below that of the reaction containing only FcH (Fig. 1).

(ii) Similar results were found for the aromatic reagents (pyridine, quinoline) and the amides.

(iii) While small amounts of pyridine and quinoline (N embedded in the aromatic ring) give very high yields of products at low concentrations, the effect falls off with increased concentration.

(iv) In general at *high reagent concentrations* if the N is in the ring (quinoline, pyridine) yields are lower than if the N is external to an aromatic ring (aniline, benzylamine).

(v) Addition of methyl groups to a carbon chain appears to give reduced CNT yields at 1% reagent addition (compare butylamine and isopropylamine; dimethylformamide and dimethylacetamide; benzylamine with *N*-benzylmethylamine). This result is consistent with the reduced yields formed when Fe alone was used *i.e.* as the C/N ratio increases the yield decreases.

(vi) Butylamine and diethylamine that have the same molecular mass, but different structures, give very similar results.

(vii) The one anomalous result relates to the use of the hexamethylenediamine (Fig. 1) where a steady increase in yield was observed with increase in reagent content. This could relate either to the coordination ability of the amine or to the chain length linking the two amine moieties.

Samples sent for CHN analysis indicated an N content of <0.5 at.% N even when the highest concentrations of N containing reagents were used (8% amine). This is consistent with recently reported data for toluene/FcH/benzylamine mixtures [30]. It was not possible to quantify the N content of the CNTs by X-ray photoelectron spectroscopy (XPS). In our previous study, we revealed that only high contents of N (>1%) can be detected by XPS [28].

In summary: with the exception of hexamethylenediamine, all the samples showed similar trends in terms of the yield with subtle differences in morphology (*i.e.* diameters and lengths as discussed below). This indicated that the source of the N is not as significant as the content of N in the reagent used to make the N-CNTs.

3.1.1. N-CNT morphology: SEM analysis

Information on the N-CNT lengths (Table 1) was obtained from SEM images and examples of the N-CNTs produced are shown in Fig. 2. The figure shows SEM micrographs of the CNTs grown by the pyrolysis of toluene/FcH in the presence of 2% and 6% formamide. All other N-CNTs synthesized in this study showed the same morphological features (Figs. S3 and S4).

Some general comments can be made from the results obtained from the range of reactions performed.

(i) The average lengths of CNTs obtained from the pyrolysis of FcH and toluene are 130 μm. This data provided a basis for comparison.

(ii) The N-CNTs grown are aligned [26b,31]. The synthesized nanotubes have uniform lengths, but the lengths vary depending on the N source.

(iii) The images reveal that the N-CNTs are not all straight.

(iv) The average lengths of all synthesized nanotubes after addition of 1% of nitrogen containing hydrocarbons are *longer* that those synthesized using toluene/FcH (Table 1). They are also better aligned and more even in distribution. This is to be contrasted with a recent study using benzylamine to produce N-CNTs [30]. As noted in our study, an increase in the nitrogen source decreases the CNT length and the study by Koos et al. reveals that if the benzylamine concentration is increased further, the tubes become even shorter. The two studies thus complement each other.

(v) The lengths shorten with increased reagent concentration. Fig. 3 shows a graphical representation of the data for benzylamine and hexamethylenediamine (see also Figs. S5 and S6 for other N containing reagents).

(vi) Growth rates of the CNTs were calculated from the lengths of the CNTs made after 45 min. While the FcH/toluene mixture gave a growth rate of 2.88 μm/min the growth rate when 1% nitrogen containing mixtures were used varied between 6.47 and 6.91 μm/min.

The rate of N-CNT growth appears to be much slower than that reported by others; reactants/conditions used in this study are however quite different from that used in earlier reported studies. For example, Ren et al. [32] synthesized large arrays of well aligned CNTs on glass using acetylene as a carbon source and ammonia gas as a catalyst and dilution gas at 700 °C. It was estimated from the TEM and SEM micrographs that the nanotubes were about 100 nm in diameter and 20 mm in length with a growth rate that was calculated to be 2 mm/min. This is about 100 times faster than the growth rates noted in this study. Kayastha et al. [33] have also synthesized N-CNTs by addition of N_2 gas to C_2H_2. These samples were grown for 15 min with an estimated length of 200 mm: A remarkable growth rate of 13 mm/min was reported.

3.1.2. N-CNT morphology: TEM analysis

The formation of MWCNTs is confirmed by TEM micrographs. A TEM image of CNTs prepared in the absence of nitrogen containing additives showed that the average outer diameter of the tubes is 55 nm. Table 1 gives the average outer diameters and average lengths

Table 1
Average diameters and length of CNTs obtained from the pyrolysis of toluene/FcH in the presence of various N containing reagents.

Reagent		1%	2%	4%	6%	8%
Diethylamine	Length (μm)	393	300	241	270	184
	Diameter (nm)	58	88	49	68	54
Butylamine	Length (μm)	444	182	172	65	111
	Diameter (nm)	78	65	73	63	61
Isopropylamine	Length (μm)	338	104	200	212	113
	Diameter (nm)	71	86	85	68	78
Pyridine	Length (μm)	393	237	175	137	111
	Diameter (nm)	54	67	48	43	37
Benzylamine	Length (μm)	518	333	245	184	226
	Diameter (nm)	66	89	100	98	85
Aniline	Length (μm)	393	325	209	205	270
	Diameter (nm)	72	107	121	90	70
N-Benzylmethylamine	Length (μm)	240	350	423	400	294
	Diameter (nm)	73	90	88	86	84
Quinoline	Length (μm)	229	306	450	278	290
	Diameter (nm)	59	95	63	52	62
1-Methylpiperazine	Length (μm)	154	182	80	96	115
	Diameter (nm)	58	79	43	50	53
Hexamethylenediamine	Length (μm)	–	271	412	388	197
	Diameter (nm)	49	51	55	59	65
N-methyethylenediamine	Length (μm)	375	92	131	86	111
	Diameter (nm)	47	52	43	56	45
Trimethylenediamine	Length (μm)	307	162	111	164	245
	Diameter (nm)	66	71	56	44	62
Formamide	Length (μm)	340	311	291	222	292
	Diameter (nm)	65	79	64	73	61
N,N-dimethylformamide	Length (μm)	300	250	323	188	153
	Diameter (nm)	51	49	62	68	65
N,N-dimethylacetamide	Length (μm)	557	235	293	354	340
	Diameter (nm)	57	52	59	66	62

FcH/toluene – no added N containing reagents: Length = 130 μm, diameter = 45 nm.

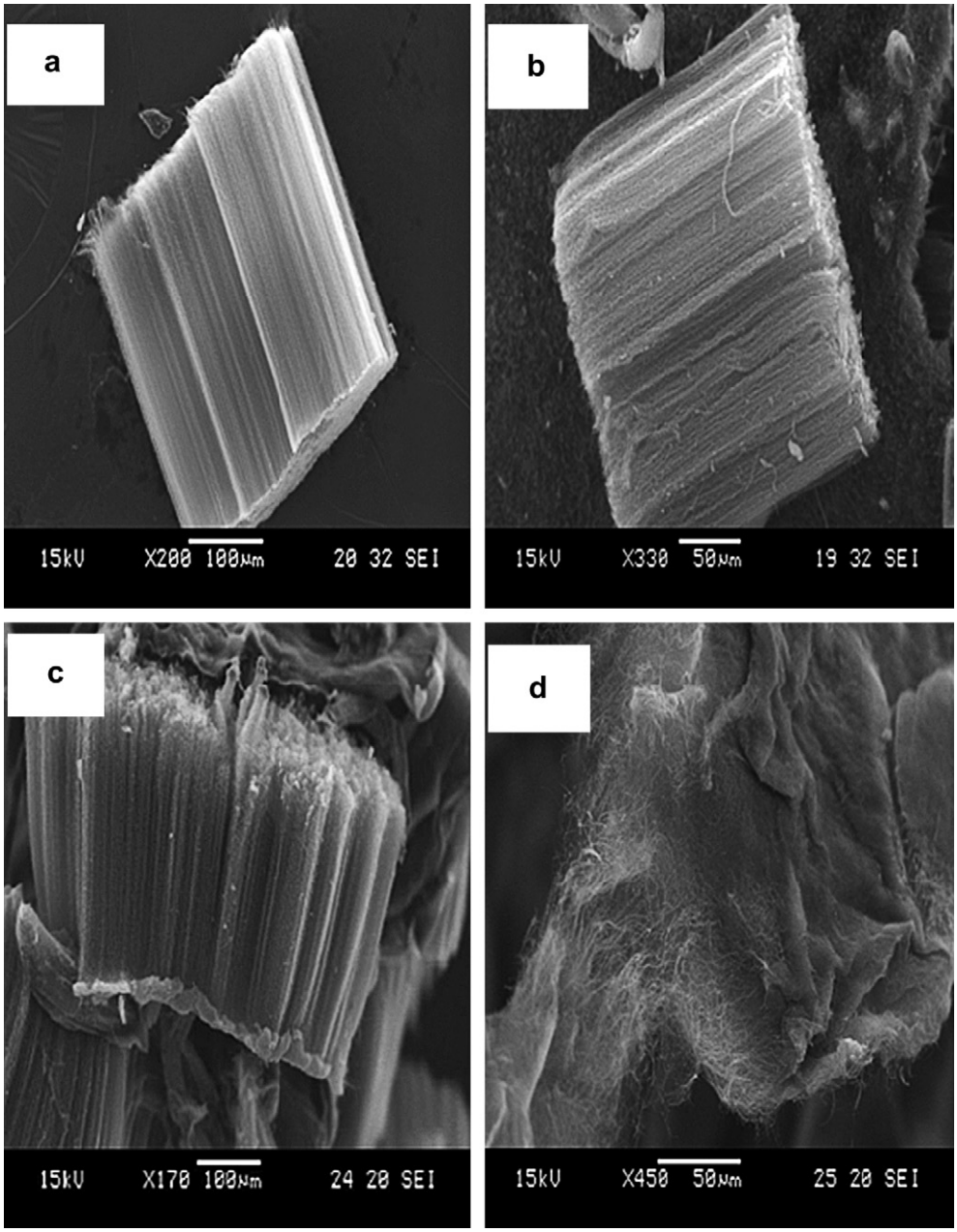

Fig. 2. SEM micrographs of CNTs obtained from the pyrolysis of toluene/FcH in the presence of (a) 2% and (b) 6% formamide; and acid treated CNTs obtained from the pyrolysis of (c) toluene/FcH and (d) toluene/FcH in the presence of 1% diethylamine.

of CNTs obtained from the pyrolysis of the nitrogen containing reagents at various concentrations. The outer diameters of N-CNTs were obtained by using the average measurement of about 50 nanotubes from at least 3 different TEM micrographs. Large tubes with diameters ranging from 40 nm to 88 nm were prepared from all the N containing reagents. Two sets of data (for benzylamine and hexamethylenediamine) are shown in Fig. 3 and Fig. S5. In every case the outer diameter was larger than that found for CNTs produced from FcH and toluene.

Fig. 4(a) shows TEM images of N-CNTs obtained by the pyrolysis of toluene/FcH in the presence of 8% diethylamine. Fig. 4(b) shows a typical TEM micrograph of an N-CNT taken at high magnification and demonstrates that indeed the tubes are of the multi-walled type. The image shows a CNT with an average diameter of approximately 49 nm. The image also reveals that the nanotubes synthesized have an expected bamboo-like structure [25,26,34]. The "bamboo-like" structure is also evident in *most* of the N-CNTs synthesized in this study.

3.1.3. Thermal analysis and Raman studies of the N-CNTs

The thermal stabilities of the various MWCNTs were evaluated by TGA analysis in air. Fig. 5(a) shows a TGA plot for CNTs obtained from the pyrolysis of toluene and FcH. The percentage residual mass, detected at $T > 700$ °C, is due to the oxidized catalyst. The CNTs did not degrade below 500 °C. The TGA plot of the CNTs prepared from FcH/toluene/8% hexamethylenediamine is depicted in Fig. 5(b) and shows that the thermal degradation commences at a temperature of 500 °C. The residual weight of nearly 7% is again attributed to oxidized catalyst nanoparticles. The CNTs are completely oxidized by 800 °C.

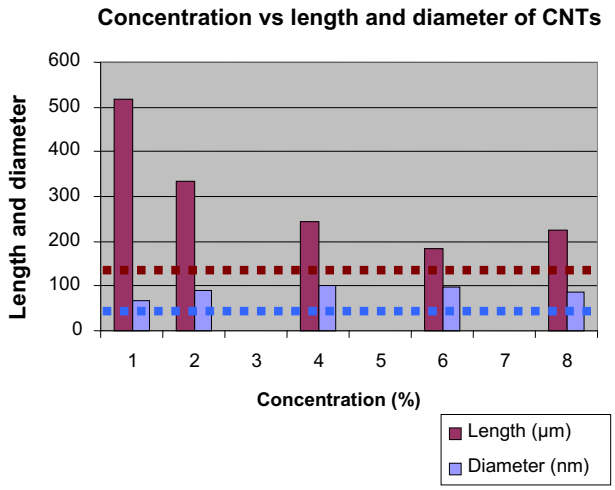

Fig. 3. Graph of concentration versus length and diameters of CNTs grown from benzylamine. Horizontal dotted line indicates lengths and diameters of CNTs obtained from FcH/toluene.

The differential TGA (DTGA) graphs showed sharp oxidation peaks between 620 and 670 °C (not shown), which are lower than the oxidative temperature for pure MWCNTs. This suggests that the N-doped CNTs are easier to oxidize than the pure MWCNTs. The mass loss maxima (obtained from the DTGA profiles) decreased from 670 to 620 °C with increasing nitrogen content in the synthesis procedure. The shift in the mass loss maxima suggests more defects and disorder in the N-CNTs.

To further investigate the graphitic nature as well as the disorder of the CNTs, Raman spectroscopy studies were performed. Fig. S9 depicts the Raman spectrum obtained from the pyrolysis of toluene/FcH in the presence of 8% diethylamine. It shows two peaks at 1356 cm^{-1} and 1585 cm^{-1}. The peak at 1585 cm^{-1} (G-band) corresponds to the high frequency E_{2g} first order mode while the D-band occurs at 1356 cm^{-1} [35]. The intensity ratios of the G-band and D-band, measured by the integration of the spectral peaks are given in Table 2. The D-band and the G-band ratio (I_D/I_G) give a measure of the graphitic nature of CNTs. A lower I_D/I_G ratio indicates a higher graphitic content of CNTs. It is clear from the data that as the concentration of diethylamine increases from 2% to 8%, the intensity ratio increases from 0.55 to 0.81 and this is attributed to an increase in the presence of defects in the CNT lattice. The intensity of the Raman spectral absorptions of tubes synthesized by pyrolysis of 2%, 4% and 8% benzylamine and isopropylamine were also recorded and their I_G/I_D ratio are shown in Table 2. In all these samples, an increase in the N source concentration results in an increase in the Raman ratio indicating an increase in the CNT disorder. There is however no straightforward correlation between the N type and N source with the Raman ratio of the CNTs.

3.2. Oxidation of N-CNTs

The effect of acid treatment on the N-CNT samples was investigated by TEM. Table S2 gives the data on the average diameter of untreated and nitric acid treated CNTs obtained by the pyrolysis of toluene and FcH. The acid treated CNTs from FcH/toluene have an average diameter of 44 nm. The diameters of the oxidized N-CNTs obtained from the pyrolysis of toluene/FcH in the presence of 1% and 8% diethylamine; 1% and 8% quinoline; 1% and 8% hexamethylenediamine; and 1% and 8% *N,N*-dimethylacetamide are also given in Table S2. It is apparent that the diameters of the treated N-CNTs obtained from the pyrolysis of diethylamine, hexamethylenediamine and *N,N*-dimethylacetamide generally *decrease* with an increase in concentration of the aforementioned nitrogen containing hydrocarbons.

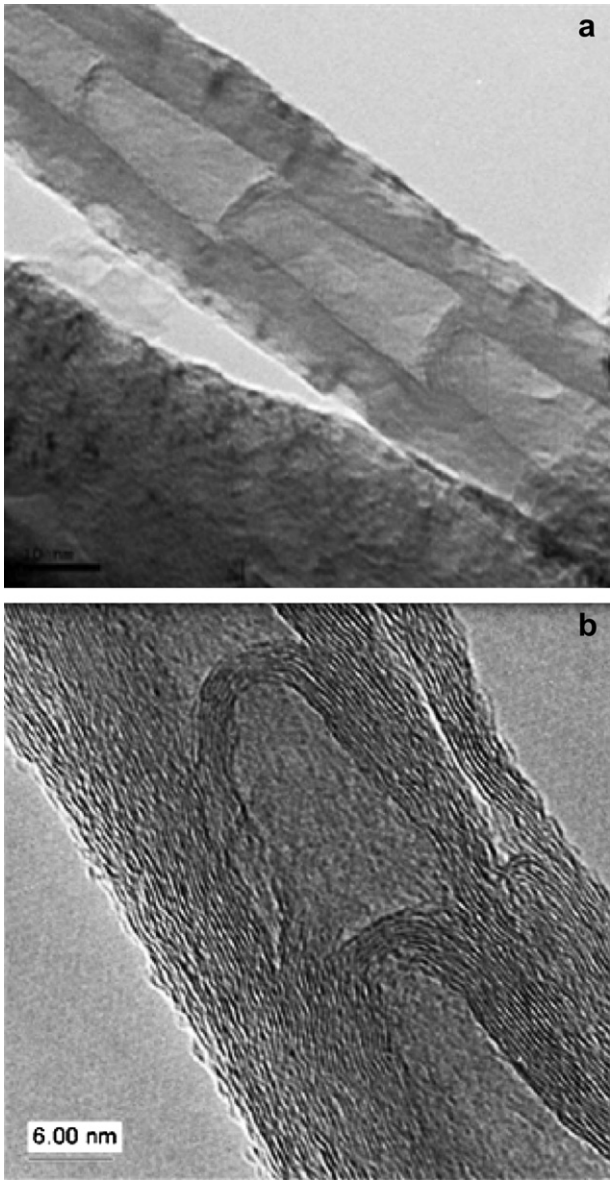

Fig. 4. TEM images of CNTs obtained from the pyrolysis of toluene/FcH in the presence of 8% diethylamine.

The SEM image of acid treated CNTs obtained from the pyrolysis of FcH and toluene is shown in Fig. 2(c). The image shows aligned CNTs with uniform length. The CNTs have an average length of 136 μm, similar to that of the untreated FcH CNTs (Table S2). Fig. 2 (d) shows the SEM images of acid treated CNTs obtained from the pyrolysis of toluene/FcH in the presence of 1% diethylamine, while Fig. S7(a) and (b) depicts SEM images of acid treated CNTs obtained from the pyrolysis of toluene/FcH in the presence of 1% and 8% hexamethylenediamine, respectively. It is evident from the images that the CNTs have lost their alignment and that the overall effect is to generate products that have a "fused/melted" look compared to untreated CNTs synthesized under similar conditions. Tubes grown from 1% to 8% quinoline (Fig. S4(a) and (b)); and 1% and 8% *N,N*-dimethylacetamide (Fig. S4(c) and (d)), show similar features.

The TGA and DTGA curves of the acid treated samples obtained under flowing air show major differences between the toluene/FcH

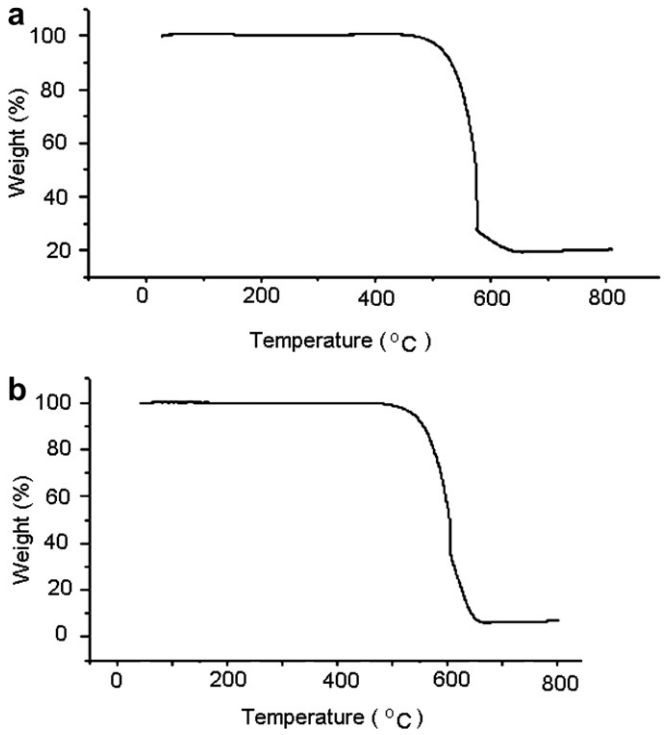

Fig. 5. TGA curve of CNTs obtained from the pyrolysis of (a) toluene/FcH; (b) toluene/FcH in the presence of 8% hexamethylenediamine.

CNTs and those synthesized by the addition of N containing reagents to the FcH/toluene solution. Decomposition occurs in the temperature range of 300–620 °C for the treated standard CNTs. It can be seen from Fig. S8(a) (for hexamethylenediamine) that the acid treated CNTs have a percentage weight loss of 94% at 620 °C, indicating increased purity after washing/oxidation (compare with Fig. 5). A two step degradation process for the treated CNTs obtained from the pyrolysis of toluene/FcH in the presence of 1% and 8% hexamethylenediamine between 300 and 610 °C is noted.

The I_D/I_G band ratio obtained from the Raman spectra of acid treated 1% and 8% diethylamine CNTs was found to be 0.52 and 0.91, respectively. These observations were related to the oxidation of the CNTs by HNO_3, which resulted in an increase in the amount of disordered carbon caused by the partial destruction of CNTs. This result suggests that the graphitization of acid treated N-CNTs prepared at low concentration of the N source is better than those prepared at higher concentrations of the N source. Thus, the data again reveals that the oxidation of N-CNTs is influenced by the N content and that the type of N source is less important in the reaction.

Table 2
I_D/I_G of CNTs obtained from the pyrolysis of toluene, FcH and N containing reagents.

Reagent	D-band	G-band	I_G/I_D
Pure (0%)	683.1	1582	0.43
Diethylamine 2%	571.9	1036.0	0.55
Diethylamine 4%	904.9	1157.6	0.78
Diethylamine 8%	1137.9	1403.1	0.81
Benzylamine 2%	740.0	1223.5	0.60
Benzylamine 4%	377.8	637.0	0.59
Benzylamine 8%	875.7	1146.9	0.76
Isopropylamine 2%	761.6	798.3	0.95
Isopropylamine 4%	609.8	735.9	0.82
Isopropylamine 8%	631.4	742.2	0.85
Isopropylamine 8%	631.4	742.2	0.85

4. Reaction mechanism

Bamboo shaped N-CNTs are proposed to form through a mechanism entailing interaction of iron clusters and C and N containing ions/radicals/atoms/clusters ('fragments') in the gas phase. At the high temperatures used, the ferrocene decomposes to form Fe atoms which cluster to form particles. At the same time, the different C and N containing reactants used to make the N-CNTs also decompose. The interaction between the Fe clusters and the C/N fragments lead to the formation of the N-CNTs.

A mechanism for the growth of bamboo N-CNTs has been proposed [36] and this mechanism can rationalize our findings. In this mechanism, the C/N fragments can either dissolve in the metal or diffuse over the metal surface. In either instance, they form a layer on the Fe particle containing C and N atoms. In the model, the C/N graphite-like layer takes the shape of the Fe particle. The presence of N in the layer is proposed to lead to stresses in the surface. This is released by a 'pulsed' effect [9,37] in which the C/N surface layer detaches from the Fe. This process is repeated over and over again leading to the bamboo shape.

In the gas phase, the type of 'fragment' formed will be influenced by the differences in the precursor used. These differences include (i) the C/N ratio of the reactant, (ii) the physical/chemical properties of the precursor and (iii) the concentration of the precursor. All of these factors will impact on the formed product. From our earlier studies on imidazoles as a source of N-CNTs [38], we also found that the structural configuration of the reactant influenced the final product.

A major conclusion from this study then is that the amount of N used is more important than the source of N used in determining the bulk yield and morphology of N-CNTs. Further analysis may still reveal subtle differences in the N-CNT structures that are due to the different N sources, but clearly these will be small effects relative to the role of the N content used to make CNTs.

5. Conclusion

We have successfully synthesized N-CNTs by a nebulised floating catalyst method using toluene and nitrogen containing reactants (1–8% mixtures) and shown the effect of employing different N containing reagent on the synthesis reactor. From the data and the discussions provided above, it is apparent that the increase in concentration of nitrogen containing hydrocarbons during the synthesis of N-CNTs results in an increase in the average outer diameter and an increase in the length of CNTs at low N concentration (<5%). The data shows that the growth rate of CNTs from the pyrolysis of toluene and ferrocene in the presence of nitrogen containing hydrocarbons *decreases* with an increase in the addition of nitrogen containing species. Increasing N content in the reactant mixture gives shorter doped tubes and tubes with more disorder. Treatment of the N-CNTs with nitric acid results in chemically modified/oxidized nanotubes with loss of alignment, decreased stability and an increased number of defects. The general conclusion is that the effects of N concentration are more important than the nature of the N source in determining the morphology and the yields of the synthesized N-CNTs.

Acknowledgements

The authors wish to thank the DST/NRF Centre of Excellence in Strong Materials, the University of the Witwatersrand and the University of Johannesburg for financial support.

Appendix. Supplementary data

Supplementary data associated with this article can be found, in the online version, at doi:10.1016/j.jorganchem.2010.08.030.

References

[1] (a) O. Stephen, P.M. Ajayan, C. Colliex, Ph. Redlich, J.M. Lambert, P. Bernier, P. Letin, Science 266 (1994) 1683;
(b) K. Suenaga, M. Yudasaka, C. Colliex, S. Iijima, Chem. Phys. Lett. 316 (2000) 365.
[2] L. Carroll, P. Redlich, X. Blase, J.C. Charlier, S. Curran, P.M. Ajayan, S. Roth, M. Ruhle, Phys. Rev. Lett. 81 (1998) 2332.
[3] B. Wang, Y. Ma, Y. Wu, N. Li, Y. Huang, Y. Chen, Carbon 47 (2009) 2112.
[4] J. Wei, H. Hu, H. Zeng, Z. Zhou, W. Yang, P. Peng, Physica E 40 (2008) 462.
[5] F.L. Deepak, N.S. John, A. Govindaraj, G.U. Kulkarni, C.N.R. Rao, Chem. Phys. Lett. 411 (2005) 468.
[6] S. Latil, F. Triozon, S. Roche, in: , NATO Science Series II: Mathematics, Physics and Chemistry, vol. 222, Springer, Dordrecht, The Netherlands, 2006, p. 143.
[7] E.N. Nxumalo, M. Mamo, A.A. Deshmukh, N.J. Coville. Oxidation of styrene using gold/nitrogen doped nanotubes, 2010, unpublished work.
[8] M.A. Mamo, F.S. Freitas, J.N. de Freitas, W.A.L. van Otterlo, A.F. Nogueira, N.J. Coville. Application of 3-hexylthiophene functionalized CNTs in photovoltaic devices, 2010, unpublished work.
[9] E.N. Nxumalo, N.J. Coville, Materials 3 (2010) 2141.
[10] C.P. Ewels, M. Glerup, J. Nanosci. Nanotechnol. 5 (2005) 1345.
[11] P. Ayala, R. Arenal, M. Rummeli, A. Rubio, T. Pichler, Carbon 48 (2010) 575.
[12] C.N.R. Rao, A. Govindaraj, Acc. Chem. Res. 35 (2002) 998.
[13] F. Villalpando-Paez, A. Zamudio, A.L. Elias, H. Son, E.B. Barros, S.G. Chou, Y.A. Kim, H. Muramatsu, T. Hayashi, J. Kong, H. Terrones, G. Dresselhaus, M. Endo, M. Terrones, M.S. Dresselhaus, Chem. Phys. Lett. 424 (2006) 345.
[14] E.J. Liang, P. Ding, H.R. Zhang, X.Y. Guo, Z.L. Du, Diamond Relat. Mater. 13 (2004) 69.
[15] R. Kurt, A. Karimi, Chem. Phys. Chem. 2 (2001) 388.
[16] C.J. Lee, S.C. Lyu, H.-W. Kim, J.H. Lee, I.C. Cho, Chem. Phys. Lett. 359 (2002) 115.
[17] M. Nath, B.C. Satishkumar, A. Govindaraj, C.P. Vinod, C.N.R. Rao, Chem. Phys. Lett. 322 (2000) 333.
[18] N. Grobert, M. Terrones, S. Trasobares, K. Kordatos, H. Terrones, J. Olivares, J.P. Zhang, Ph. Redlich, W.K. Hsu, C.L. Reeves, D.J. Wallis, Y.Q. Zhu, J.P. Hare, A.J. Pidduck, H.W. Kroto, D.R.M. Walton, Appl. Phys. A 70 (2000) 175.
[19] M. Terrones, N. Grobert, J. Olivares, J.P. Zhang, H. Terrones, K. Kordatos, W.K. Hsu, J.P. Hare, P.D. Townsend, K. Prassides, A.K. Cheetham, H.W. Kroto, D.R.M. Walton, Nature 388 (1997) 52.
[20] R. Che, L.M. Peng, Q. Chen, X.F. Duan, Z.N. Gu, Appl. Phys. Lett. 82 (2003) 3319; F.L. Deepak, A. Govindaraj, C.N.R. Rao, Chem. Phys. Lett. 345 (2001) 5.
[21] Z. Osváth, A.A. Koós, N. Grobert, Z. Vértesy, Z.E. Horváth, L.P. Biró, J. Nanosci. Nanotechnol. 9 (2009) 6139.
[22] P. Ghosh, M. Tanemura, T. Soga, M. Zamri, T. Jimbo, Solid State Commun. 147 (2008) 15.
[23] (a) V. Bajpai, L. Dai, T. Ohashi, J. Am. Chem. Soc. 126 (2004) 5070;
(b) R. Sen, B.C. Satishkumar, A. Govindaraj, K.R. Harikumar, M.K. Renganathan, C.N.R. Rao, J. Mater. Chem. 7 (1997) 2335.
[24] (a) P. Ghosh, T. Soga, K. Ghosh, R.A. Afre, T. Jimbo, Y. Ando, J. Non-Cryst. Solids 354 (2008) 4101;
(b) S. Maldonado, S. Morin, K.J. Stevenson, Carbon 44 (2006) 1429;
(c) J. Feng, Y. Li, F. Hou, X. Zhong, Mater. Sci. Eng. A 473 (2008) 238.
[25] (a) R.M. Yadav, P.S. Dobal, T. Shripathi, R.S. Katiyar, O.N. Srivastava, Nanoscale Res. Lett. 4 (2009) 197;
(b) R.M. Yadav, D.P. Singh, T. Shripathi, O.N. Srivastava, J. Nanopart. Res. 10 (2008) 1349.
[26] (a) J. Jiang, T. Feng, X. Cheng, L. Dai, G. Cao, B. Jiang, X. Wang, X. Liu, S. Zou, Nucl. Instrum. Meth. B 244 (2006) 327.(b) C.J. Lee, J. Park, Appl. Phys. Lett. 77 (2000) 3397.
[27] S. Trasobares, O. Stephan, C. Colliex, W.K. Hsu, H.W. Kroto, D.R.M. Walton, J. Chem. Phys. 116 (2002) 8966.
[28] E.N. Nxumalo, V.O. Nyamori, N.J. Coville, J. Organomet. Chem. 693 (2008) 2942.
[29] S.R.C. Vivekchand, L.M. Cele, F.L. Deepak, A.R. Raju, A. Govindaraj, Chem. Phys. Lett. 386 (2004) 313.
[30] A.A. Koós, M. Dowling, K. Jurkschat, A. Crossley, N. Grobert, Carbon 47 (2009) 30.
[31] D.Y. Zhong, S. Liu, G.Y. Zhang, E.G. Wang, J. Appl. Phys. 89 (2001) 5939.
[32] Z.F. Ren, Z.P. Huang, J.W. Xu, J.H. Wang, P. Bush, M.P. Siegal, P.N. Provencio, Science 282 (1998) 1105.
[33] V. Kayastha, Y. Yapa, K.S. Dimovski, Y. Gogotsi, Appl. Phys. Lett. 85 (2004) 3265.
[34] H. Liu, Y. Zhang, R. Li, X. Sun, S. Desilets, H. Abou-Rachid, M. Jaidann, L.-S. Lussier, Carbon 48 (2010) 1498.
[35] M. Kohno, T. Orii, M. Hirasawa, T. Seto, Y. Murakami, S. Chiashi, Y. Miyauchi, S. Maruyama, Appl. Phys. A 79 (2004) 787.
[36] M. Terrones, A.M. Benito, C. Manteca-Diego, W.K. Hsu, O.I. Osman, J.P. Hare, D.G. Reid, H. Terrones, A.K. Cheetham, K. Prassides, H.W. Kroto, D.R.M. Walton, Chem. Phys. Lett. 257 (1996) 576.
[37] C.T. Wirth, S. Hofmann, J. Robertson, Diamond Relat. Mater. 18 (2009) 940.
[38] E.N. Nxumalo, V.P. Chabalala, V.O. Nyamori, M.J. Witcomb, N.J. Coville, J. Organomet. Chem. 695 (2010) 1451.